MTP-217

COMMUNICATIONS AT MILLIMETER WAVES

A. K. Kamal and P. F. Christopher

The MITRE Corporation
Bedford, Massachusetts

ABSTRACT

The advantages and disadvantages of millimeter waves for terrestrial and satellite communications are discussed. Atmospheric attenuation is discussed in detail; signal loss in particulates, sandstorms, snow, hail, and fog are treated briefly. Then, short closed forms are found for gaseous attenuation on ground-satellite paths. An exponential rain loss probability density function is used to generate atmospheric loss at arbitrary required availability. This loss (as a function of frequency) can be used to pick optimum carrier frequencies as a function of location, required availability, elevation angle, and system cost.

An estimate of the rate-of-change of millimeter wave device availability is made. GaAs FETs receive special attention, not only because they will be useful, but because one phase of their millimeter wave performance is predictable: their noise performance as a function of frequency can be estimated with the aid of a Fukui equation. Their performance as a function of time can be lower bounded by a relation due to Block and Galage. The 30/20 GHz satellite bands are estimated to be commercially useful by 1985.

FOREWORD

This paper is similar to the one presented by the authors at the 1981 International Conference on Communications, held on June 14-18, 1981, at Denver, Colorado.

ACKNOWLEDGMENTS

TABLE OF CONTENTS

LIST OF ILLUSTRATIONS

SECTION 1

INTRODUCTION

A fair amount of thought is currently being given towards the possible applications of the millimeter wave spectrum for communications. Workers in the general field of microwaves are apprehensive about pushing towards EHF frequencies, mainly because of atmospheric attenuation and higher component costs. The interest in millimeter waves is well justified due to the ever increasing demand for extremely wide system bandwidths that allow more data transfer and smaller size components. The relatively small size of antennas provides sharp collimated beams. The tremendous progress in solid-state technology has resulted in very small subsystems in transmitters and receivers. These size reductions have greatly helped the mobility due to lightweight systems. On the side of transmitted power outputs, hope is renewed every day that sufficient power would be available for most of the applications. The advances made in solid-state technology and microwave integrated circuits have been responsible for achieving significant power generation. Special mention may be made of the techniques called power combining and space combining. The strong attenuation due to oxygen absorption especially at 60 GHz, although detrimental to relatively long range communications, is extremely effective for certain applications such as covert communications, due to the limit it imposes on the unwanted detection range. The low attenuation windows around 35, 94, 140, and 230 GHz can be used with best possible results in achieving the

1

maximum range. A hybrid optical fiber millimeter wave communication system seems to be extremely attractive; the millimeter wave system is in the line-of-sight (LOS) section.

Millimeter wave propagation is not without pitfalls. Severe attenuation due to oxygen absorption occurs at a few frequencies, such as 60 GHz. Fortunately the oxygen absorption line is so sharp that operating at frequencies about 10 GHz above or below the absorption line would be in a region of little attenuation due to oxygen. The rain attenuation is one of the most important factors that limits the reliability due to significant attenuation during heavy rain. Above 100 GHz the rain attenuation curve flattens out. Hence in the design and implementation of communication systems at millimeter waves, attenuation due to rainfall becomes the major atmospheric effect. Other causes of attenuation, although not very significant up to 150 GHz, include fog, snow, hail, and even heavy sandstorm. The attenuation due to fog, for example, becomes important at 400 to 500 GHz. For applications where the attenuation due to rain and oxygen is either very small or nonexistent, such as from aircraft to satellite or from satellite to satellite, millimeter wave communication systems offer interesting solutions.

SECTION 2

BACKGROUND

The ever increasing satellite communications system requirements, in addition to the frequency congestion and management problems at microwaves and lower frequencies, have directed the attention of workers in this field toward the use of millimeter waves for communications. With the tremendous progress in solid-state technology, and hence the development of microwave integrated circuits (MIC), it is now possible to have millimeter wave components and subsystems with production quality. Although the atmospheric effects resulting in attenuation are more pronounced at these frequencies, there are low attenuation windows centered around 35, 94, 140, and 230 GHz that can be used to substantial effective ranges. On the other hand, the high attenuation due to the oxygen absorption line at 60 GHz (frequency dependent attenuation) can be used to provide the possibility of good covertness, due to very limited signal overshoot. The smaller antenna aperture requirements, better spatial resolution, and small components and subsystems, besides wider bandwidth and higher data rates, give millimeter wave systems many advantages over the microwave systems.

Frediani[1] and later on Cummings et al.,[2] have considered the current and projected needs of satellite communications in both civil and military areas. They have addressed many factors such as frequency bands, propagation effects, terminal antenna gain limitation, effective radiated power, and low probability of interception. They concluded that it would be more advantageous to design and operate a communication system at EHF

3

rather than at SHF or lower frequencies. For the military applications, the EHF becomes all the more attractive because of increased bandwidth and better antijam protection, beside the improved low probability of interception (LPI). A reasonably developed technology base is being promised at present, and by the time a communication system becomes operational, there would be no question of obtaining all that is basically required.

A totally new dimension in information carrying capacity came into the limelight with the advent of fiberoptic transmission. Advantages include secure communications, freedom from electromagnetic interference (EMI), radio frequency interference (RFI), and electromagnetic pulse (EMP) effects caused by lightning, radio and radar stations, and nuclear events, respectively. Outside interferences from electromagnetic sources as well as the problem of fading or other atmospheric effects are nonexistent in optical fiber communications. However, there are many situations where the terrain difficulties would make the laying of optical fiber cables nearly impossible. Also, these cables can be cut or destroyed if they happen to be in the path of unfriendly vehicles. In addition, it is inconceivable that in a troubled arena, one can lay such cables and still have survivable communications. Since optical transmission in the atmosphere would suffer from attenuation due to fog, smoke, or from most of the particulate matter, attention is being directed towards the millimeter wave communication system, especially for short distances on the order of about 10 km. It is also logical to consider systems presenting a hybrid optical fiber–millimeter wave solution. The millimeter wave would be the line–of–sight (LOS) open space section.

In any communication system employing the atmosphere as the transmission medium, there are problems of multipathing which can be caused by

a number of factors. In millimeter wave communication systems, the change in signal level due to multipath fading needs further consideration. Some experimental studies have been performed but the results are far from conclusive. Generally, extrapolation of the results obtained in the frequency range of 4 to 6 and 8 to 11 GHz were described in literature. However, there are specific problems such as the peculiarities of propagation, rain attenuation, and highly directed antenna beam which should be considered separately.

Ruthroff[3] gave an expression for a no-fade path distance L_o as:

$$L_o \approx 4.8\lambda^{1/3} \text{ kilometers, } \lambda \text{ in cm} \qquad (1)$$

This expression is approximate, since it is based on two-ray theory and on some of the extrapolations based on 4 to 6 GHz experiments. As a matter of fact, the multipath fading is a function of a number of variables associated with atmospheric conditions, such as antenna beamwidth, path length, and the season. The time of the day also plays a very important role. Several techniques such as space, frequency, and even angle diversity are available to combat the fading due to multipathing.

In the area of earth-satellite communication systems, millimeter waves are becoming extremely attractive due to high data rate capability, minimum interference from terrestrial LOS systems, high achievable gain with narrow beam widths of small antennas, and the availability of usable spectrum. As a matter of fact, CCIR has already made tentative frequency allocations for all the millimeter wave spectrum; and in atmospheric windows, the uplink and downlink assignments are being proposed. It is also possible to obtain reliable millimeter-wave components and systems, although at increased costs. With improved technologies, the cost factor would become quite

attractive; one can look forward to years ahead when the millimeter wave hardware will compete favorably with hardware at lower frequencies. In the future, as the solid-state technology advances, more power output will be available so that with the advantages of millimeter waves including mobility, the earth terminals at these frequencies will be preferred.

SECTION 3

FACTORS AFFECTING PROPAGATION

Millimeter wave propagation is subject to losses due to a number of factors resulting in absorption, scattering, reflection, and/or refraction. In recent years, extensive studies have been directed at determining the effects on millimeter wave transmission of atmospheric gases, rain, water vapor, hail, snow, clouds, fog, and even sandstorms.

The molecular absorption of millimeter wave energy by oxygen and water vapor is responsible for producing a series of molecular resonance absorption peaks at various frequencies. The two factors that really pose problems in designing a communication system are oxygen and precipitation which cause attenuation.

Millimeter wave absorption by oxygen, which depends on frequency and altitude, is due to a band of molecular magnetic dipole rotational transitions with resonant frequencies around 60 GHz and 120 GHz.

Depending on the drop size, density, and the statistical distribution of the drops during rain, one can estimate the rain attenuation for a millimeter wave path. It is possible to consider small displacement currents set up in hydrometers resulting in scattering and absorption. The scattering may give rise to interference between two or more millimeter wave paths, and absorption is directly responsible for the signal loss.

3.1 ATTENUATION BY SNOW AND HAIL

Generally for frequencies below 100 GHz, the attenuation caused by snow and hail is significantly less than the attenuation due to rain. This is due to the fact that the dielectric constant of ice is much smaller than water and produces smaller scattering cross sections of snow (snowflakes, ice needles) and hailstorms. It is worth noticing that in the case of wet snow, the scattering cross section may be larger than that of dry snow. The specific attenuation will still be approximately proportional to the mass of liquid water. Furthermore, the ice flake or even hail abosrbs much less millimeter wave energy than a comparable rain drop. There can be a few climatic regions where the attenuation due to hail at millimeter wave frequencies can be significant. However, this may happen for a very small percentage of time on the order of 0.001 or less.

3.2 ATTENUATION BY FOG OR CLOUDS

For attenuation caused by fog or clouds, it is assumed that the water content is of the order of 0.25 g/m^3, giving rise to attenuation which is not significant compared to rain. However, as the liquid water content becomes high (1-5 g/m^3), as in dense fog,[4] the attenuation starts to become comparable to rain, especially above 50 GHz.

3.3 ATTENUATION DUE TO SAND AND DUST STORMS

Although there is a dearth of research and publications in this area, it can be safely assumed that most of the signal loss is due to scattering and none to absorption. For dust and sand particle concentrations of 10^{-5} g/m^3, the attenuation[5] is about 0.4 dB/km. In severe sand storms and at higher operating frequencies of millimeter wave range, the signal

attenuation can be appreciable, especially for the ground-to-ground links. The extent of sandstorm path may be between 2 to 3 km and hence the signal loss is expected to be 2 to 3 dB.

The two factors that affect the millimeter wave propagation most are 1) attenuation due to atmospheric gases, especially oxygen, and 2) attenuation due to rain. We discuss these two factors further and bring out some interesting results, especially for ground-to-satellite communications.

3.4 GASEOUS ATTENUATION

J. H. Van Vleck[6] has considered the quantum-mechanical formula for 0_2 absorption of microwaves at great length. An approximation he made, for a radio frequency less than 30 GHz, for the sum of many individual absorption lines appears again in an analysis by Bean and Dutton.[7] Bean and Dutton[7] show Van Vleck's expression as valid up to 50 GHz; the first approximation to oxygen attenuation in decibels per kilometer, γ_1, is shown as:

$$\gamma_1 = \frac{0.34}{\lambda_c^2} \left[\frac{\Delta\nu_1}{\frac{1}{\lambda_c^2} + \Delta\nu_1^2} + \frac{\Delta\nu_2}{\left(2 + \frac{1}{\lambda_c}\right)^2 + \Delta\nu_2^2} \right.$$

$$\left. + \frac{\Delta\nu_2}{\left(2 - \frac{1}{\lambda_c}\right)^2 + \Delta\nu_2^2} \right] \text{dB/km at standard atmospheric pressure}$$

(2)

where

$$\Delta\nu_1 = 0.018 \text{ cm}^{-1} \text{ atm}^{-1}$$

9

and

$$\Delta \nu_2 = 0.049 \text{ cm}^{-1} \text{ atm}^{-1}$$

$$\lambda_c = \text{wavelength in cm}$$

are seen to depend linearly on atmospheric pressure. In addition, Bean and Dutton[7] chose to change the intensity factor $(0.34/\lambda_c^2)$ at the front of the equation (2) to:

$$\left(\frac{0.34}{\lambda_c^2}\right)\left(\frac{P}{1013.25}\right)\left(\frac{293}{T}\right)^2 \tag{3}$$

where atmospheric pressure, P, is in millibars and temperature, T, is in degrees kelvin (K). This in turn causes the intensity factor to be linearly pressure dependent, so that both the amplitude and shape of the absorption curve are changing with pressure (altitude). If one further lets atmospheric pressure be an exponential function of altitude

$$P \text{ (atmospheres)} = \exp\left(-h/H_o\right)$$

one can see how the magnitude and shape of equation (2) changes with altitude. Temperature is a second order effect and its variation is omitted in the following development. H_o is the scale height and is typically 7 to 8 km.

We are interested in total gaseous attenuation on a ground-to-satellite path. When oxygen attenuation (dB/km) is integrated from altitude, h, to infinity, and if one assumes that gaseous path length is proportional to the

10.

cosecant of elevation angle, one finds that the Van Vleck O_2 equation can be integrated to yield:

$$A_{0_2} = \frac{0.34}{\lambda_c^2} \left(\frac{-H_o}{\sin E} \right) \left\{ \left(\frac{1}{2K_1} \right) \ell n \left(\frac{\frac{1}{\lambda_c^2}}{\frac{1}{\lambda_c^2} + K_1^2 v_1^2} \right) + \left(\frac{1}{2K_2} \right) \ell n \left[\frac{\left(2 + \frac{1}{\lambda_c} \right)^2}{\left(2 + \frac{1}{\lambda_c} \right)^2 + K_2^2 v_1^2} \right] + \left(\frac{1}{2K_2} \right) \ell n \left[\frac{\left(2 - \frac{1}{\lambda_c} \right)^2}{\left(2 - \frac{1}{\lambda_c} \right)^2 + K_2^2 v_1^2} \right] \right\}$$

(4)

where A_{0_2} is total oxygen attenuation (dB) (1 GHz < f < 50 GHz). Total oxygen attenuation is also useful on a ground-satellite link where

$$K_1 = 0.018$$

$$K_2 = 0.049$$

$$V_1 = \exp \left(-h_1/H_o \right) ; \quad h_1 = \text{ground station altitude, km} .$$

The constant scale height, H, which appeared in both the intensity and line width portions of γ_1 allowed this fast, closed form integration. However, the analogous situation does not exist for water vapor; the scale height for water vapor content is about 2 km, but the scale height of line width is H_o (7 or 8 km).

11

A short result can also be found for integrated water vapor attenuation if the water vapor scale height is assumed to be exactly $(H_o/4)$. The result for integrated water vapor attenuation is:

$$A_{H_2O} = \left(\frac{0.0035}{\lambda_c^2}\right) \frac{\rho_o}{K_3} \left(\frac{H_o}{\sin E}\right) \times \left\{ \frac{2v_1^3}{3} - \frac{a_1}{K_3^2} \times \left(v_1 - \frac{\sqrt{a_1}}{K_3} \tan^{-1} \frac{K_3 v_1}{\sqrt{a_1}}\right)\right.$$

$$\left. - \frac{a_2}{K_3^2} \left[v_1 - \frac{\sqrt{a_2}}{K_3} \tan^{-1}\left(\frac{K_3 v_1}{\sqrt{a_2}}\right)\right] \right\} \quad \text{dB } H_2O \text{ attenuation}$$

$$(5)$$

where

$$K_3 = 0.087$$

$$v_1 = \exp\ (-h_1/H_o)$$

$$a_1 = \left(\frac{1}{\lambda_c} - \frac{1}{1.35}\right)^2$$

$$a_2 = \left(\frac{1}{\lambda_c} + \frac{1}{1.35}\right)^2$$

ρ_o = water vapor density at the earth's surface, g/m^3.

The total attenuation, A, on a ground-satellite link due to both the oxygen and water vapor absorption can now be found by simply adding A_{O_2} and A_{H_2O}. These two equations give the shortest general total attenuation

relations of which we are aware. At least an order of magnitude of computer time can be saved by using these relations and avoiding conventional numerical integrations. The gaseous attenuation integrated over exponential atmosphere vs. frequency is shown in figure 1.

3.5 RAIN ATTENUATION

Rain attenuation may often be treated as a two-parameter exponential probability density function. This is apparent in a form of the Rice Hulmberg relations for attenuation given by Dutton,[7] and the exponential function has been useful in other derivations.[8] For example, constant elevation angle experiments conducted with Applications Technology Satellite-6 (ATS-6) were quantitatively different at each ground location, but they would be represented approximately by

$$ P \left(A_R \geq A \right) = \phi \ \exp \ - \frac{(A - \lambda)}{\beta} \ , \quad \text{for} \quad A \geq \lambda $$

where rain attenuation $A_R \geq$ an arbitrary attenuation A, dB

ϕ = fraction of time noticeable rain or cloud attenuation occurs

λ = lower cut-off for exponential distribution, dB

β = standard deviation of exponential distribution, dB.

We assume that λ and β can be weighted by (csc elevation) so that equation (5) can apply to other elevation angles. We also assume that attenuation goes as frequency raised to some power.
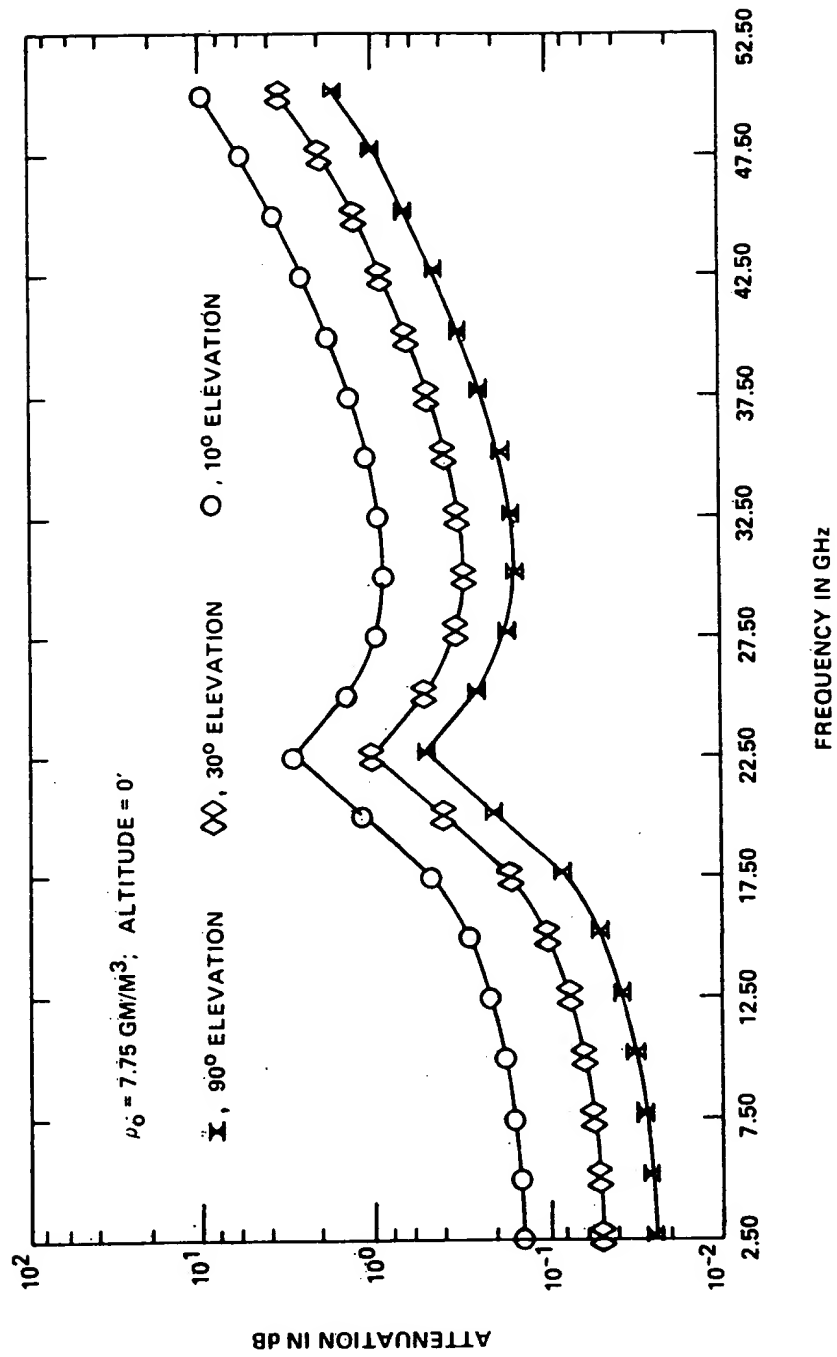
13

Figure 1. Gaseous Attenuation Integrated Over Exponential Atmosphere

The equivalent β at some new frequency, f_o GHz, and some elevation angle, E, is found at:

$$\beta' = \beta \left(\frac{f}{f_o}\right)^\zeta \left(\frac{\sin E_o}{\sin E}\right), \qquad \text{dB for } E > 10^o \qquad (7)$$

and

$$\lambda' = \lambda \left(\frac{f}{f_o}\right)^\zeta \left(\frac{\sin E_o}{\sin E}\right), \qquad \text{dB for } E > 10^o \qquad (8)$$

where f_o and E_o are reference parameters for λ, β.

The more severe attenuation losses at frequencies higher than f GHz are handled automatically by using λ' and β' for the two-parameter exponential distribution. One good means for combatting rain losses is a simple switched diversity system with ground stations separated by 20 to 30 km. If this separation can give independent rain losses, the resultant rain loss distribution can be found by taking that station (of m stations) which suffers minimum loss. This switched diversity gives another simple result:

$$P_m \left(A_R \geq A\right) = \left[\Phi \, \exp - \frac{(A - \lambda')}{\beta}\right]^m, \quad \text{for} \quad A \geq \lambda'$$

$$= \Phi^m \, \exp - \frac{(A - \lambda')}{\beta'/m} \quad . \qquad (9)$$

This can easily be solved for any P_m, which is an overwhelming advantage over graphical techniques.

Figure 2 shows the rain rate climate regions of the United States. One frequency choice of interest would occur in the heavy rain region of Florida (region E).

A new rain model by R. K. Crane is undergoing favorable review as a strong possibility to replace old CCIR rain models. A thorough outline of many parameters is presented in graphical form in refs. 9 and 10 and not repeated here. The frequency dependence is also presented in graphical form; however, when it is examined in detail as a functional form, it can be found to show a $f^{2.45}$ power relation between 10 GHz and 40 GHz. Bell Labs researchers ranging from Wilson[11] to recent contributors, Reudink[9] and others, have shown nearly an f^2 dependence for attenuation. Office of Telecommunication researchers such as Dutton have also used f^2. Other valuable research[10] has indicated exponents as low as 1.72.

Early validation tests on Crane's model have been successfully run at 15 GHz. It is probable that tests at 40 GHz will require an exponent close to 2.0. Therefore, Crane's model is implemented directly in figures 3 through 6, except for the frequency exponent which is set equal to 2.0. Elevation angles are shown in degrees. A bi-exponential distribution (two straight line segments on semi-log paper) is used to represent Crane's rainfall statistics.

It is seen from figures 4 and 6 that diversity is not only a powerful method for coping with rain losses, but optimum frequencies shift sharply upward.
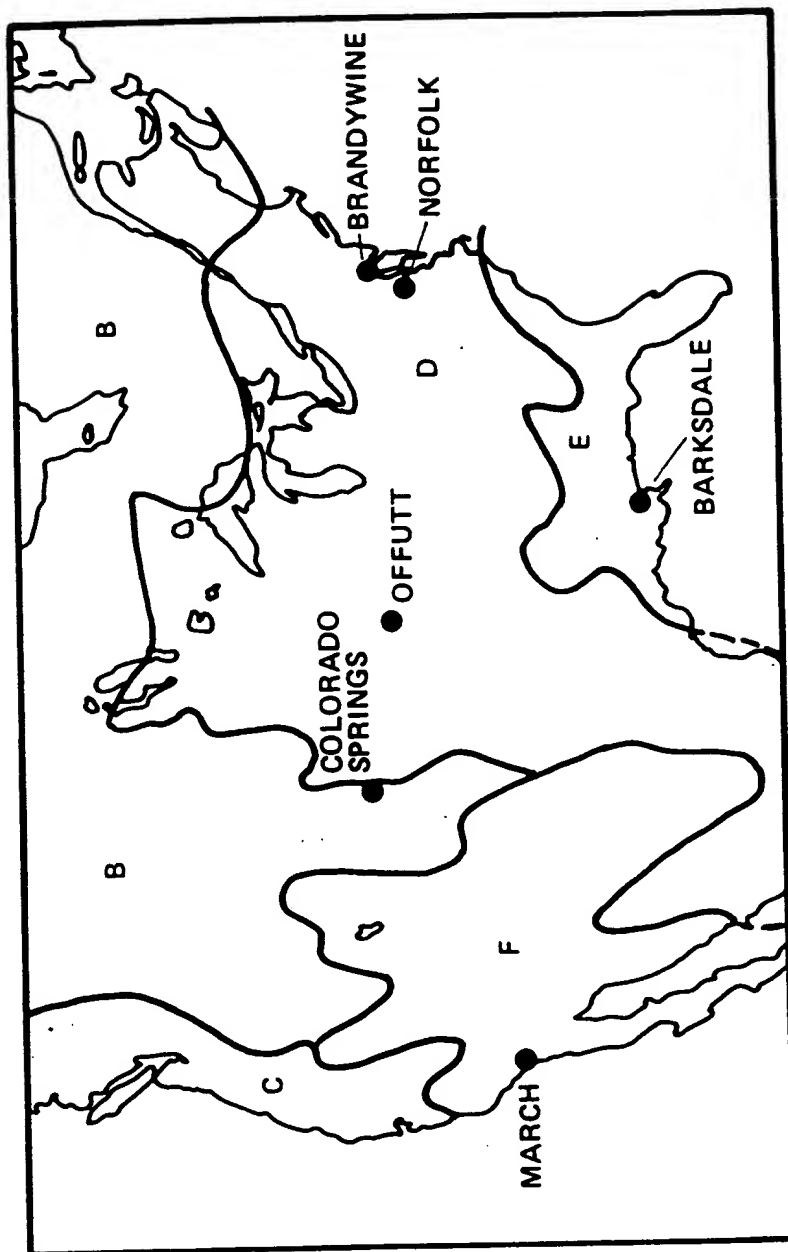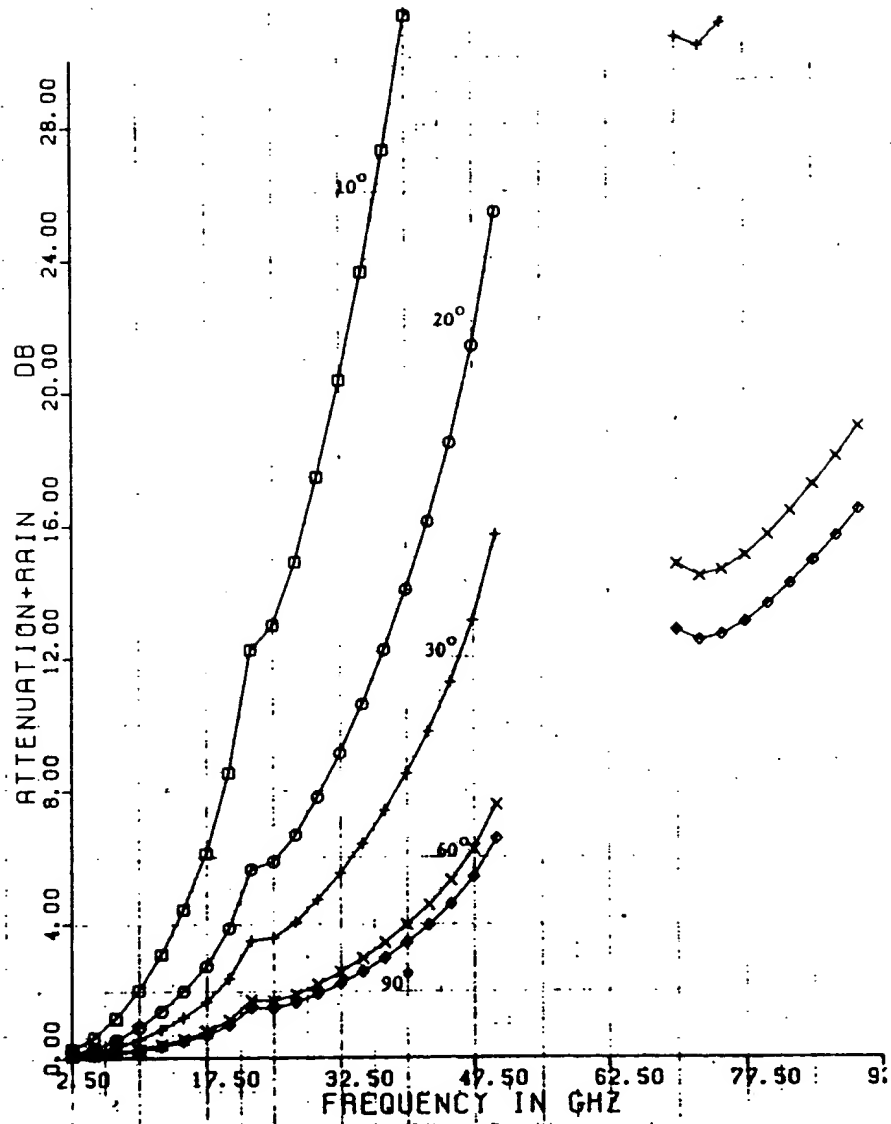
Figure 2. Rain Rate Climate Regions

17

Figure 3. Gaseous Attenuation + Rain vs. Frequency,
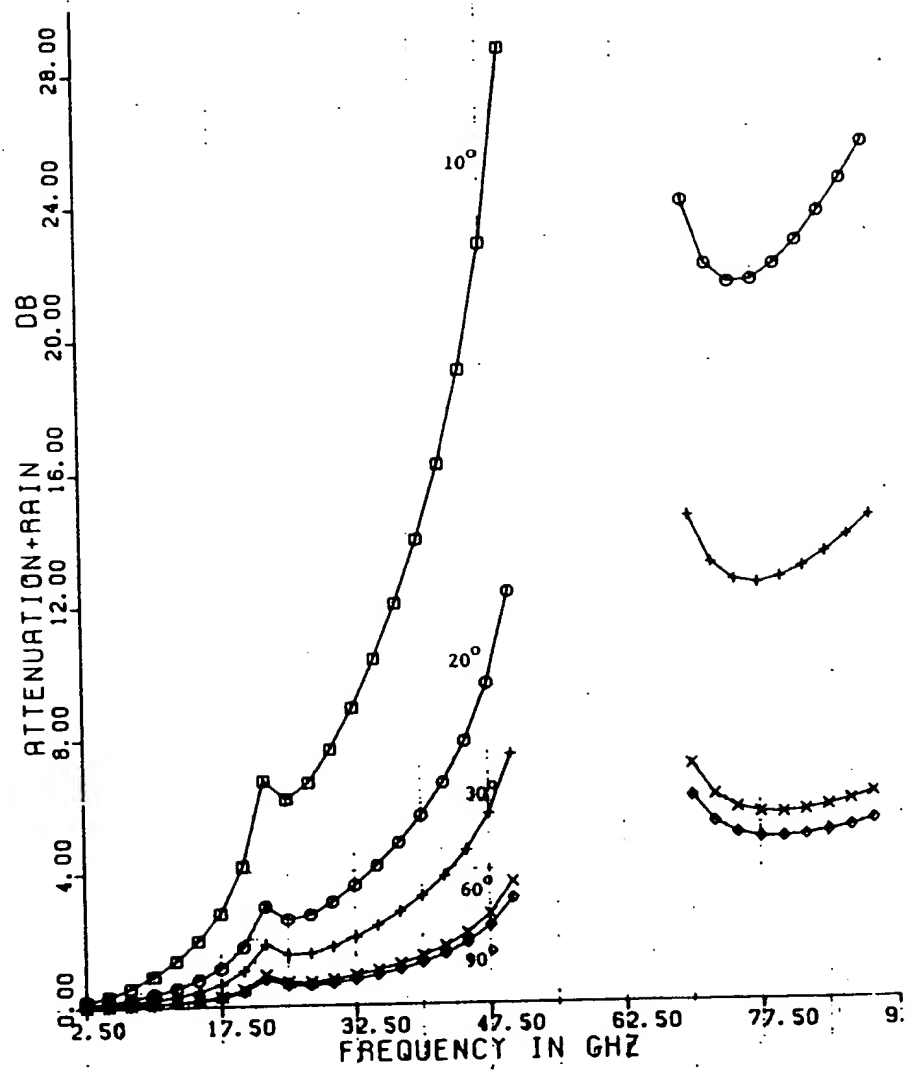0.99 Availability, Region E

18

Figure 4. Gaseous Attenuation + Rain vs. Frequency
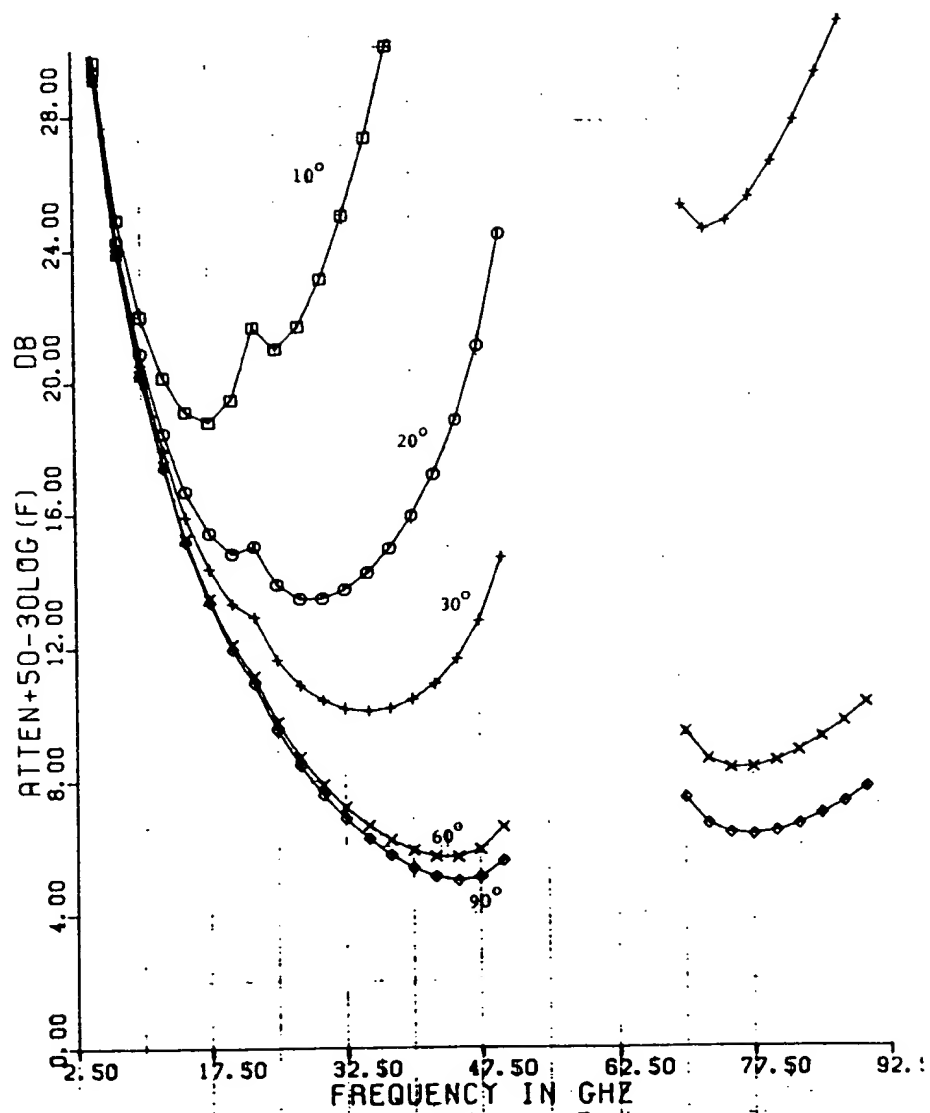0. 99 Availability, Dual Diversity, Region E

19

Figure 5. Attenuation – Gain + Interference (for Frequency
Which Minimizes I/S), 0. 99 Availability, Region E
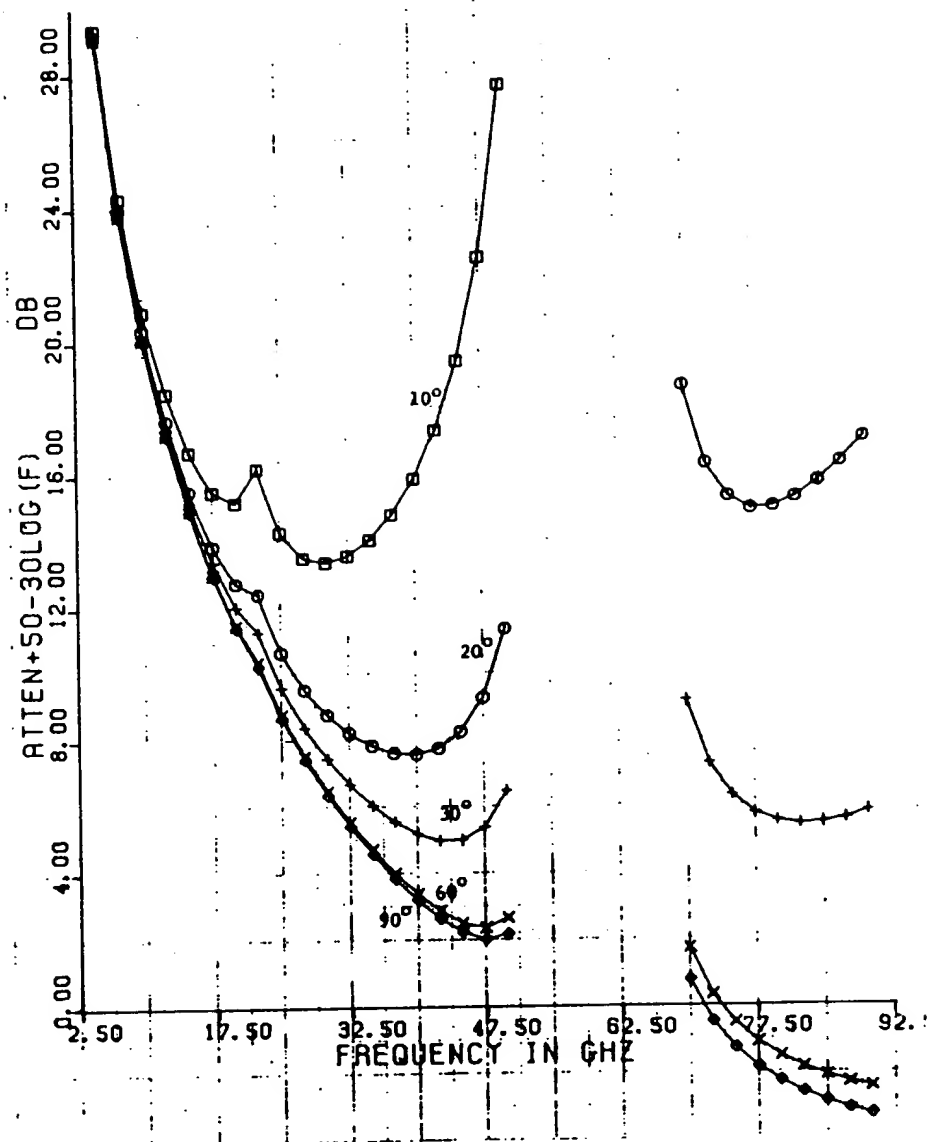
20

Figure 6. Attenuation – Gain + Interference (for Frequency Which
Minimizes I/S), 0. 99 Availability, Dual Diversity, Region E

21

If only modest availability (0.99) is required, a rain rate of 4 mm/hr is used to generate figures 3 and 4. A 5.5 dB attenuation is suffered at 32.5 GHz and at 30° elevation for the single ground station of figure 3. We are concerned with 30° elevation (and higher) because our experience[12] suggests that 30° elevation angle can usually be available in a well designed satellite system. Attenuation of 2 dB is shown on figure 4 when two independent ground stations are available, with switched diversity.

One advantage of millimeter wave (vs. microwave) frequencies is the ability to discriminate against interference sources which are outside the main beam. Not only does the main beam gain increase with frequency, but the sidelobe envelope drops (even for a uniformly illuminated dish — which is one of the worst illuminating patterns for lobes). Another f^1 advantage accrues against the interference source, so if we are concerned with maximizing (signal/interference), we plot attenuation $-30 \log_{10} f$ (E region), see appendix.

Figures 5 and 6 show these plots for the Florida region. A single ground site (figure 5) suffers minimum interference-to-signal loss at 35 GHz and 30° elevation. If two independent ground sites are available as in figure 6, the best frequency increases to 42 GHz. But surprisingly, a frequency region approaching 90 GHz starts to become competitive. This is a region of interest for a fiber optic/millimeter wave transition.

SECTION 4

DEVICE AVAILABILITY

We have shown some propagation characteristics of millimeter waves which imply that they can be useful and even attractive for further study. The fruition of these areas, however, will depend on the availability of reliable, inexpensive power sources, amplifiers, receivers, and antennas. Those developments have been occurring so quickly in the past few years that we must be concerned not only with present devices, but the rate of change of these devices. The rate of change has been quantified in one related technology area (computers), and we will use a rate-of-improvement relation which has been successfully applied to solid state devices for computers.

4.1 LOW NOISE AMPLIFIERS

One appropriate place to start a state-of-the-art discussion is in a very promising and rapidly advancing technology. GaAs FET's are not only moving into production status but are expected to improve further in the near future. The rate of change of solid state devices can be estimated in the 1978-1985 period, and checked for the 1978-1980 period. Figure 7 shows data points for existing devices. The curves are generated by a means given by H. Fukui.[14]
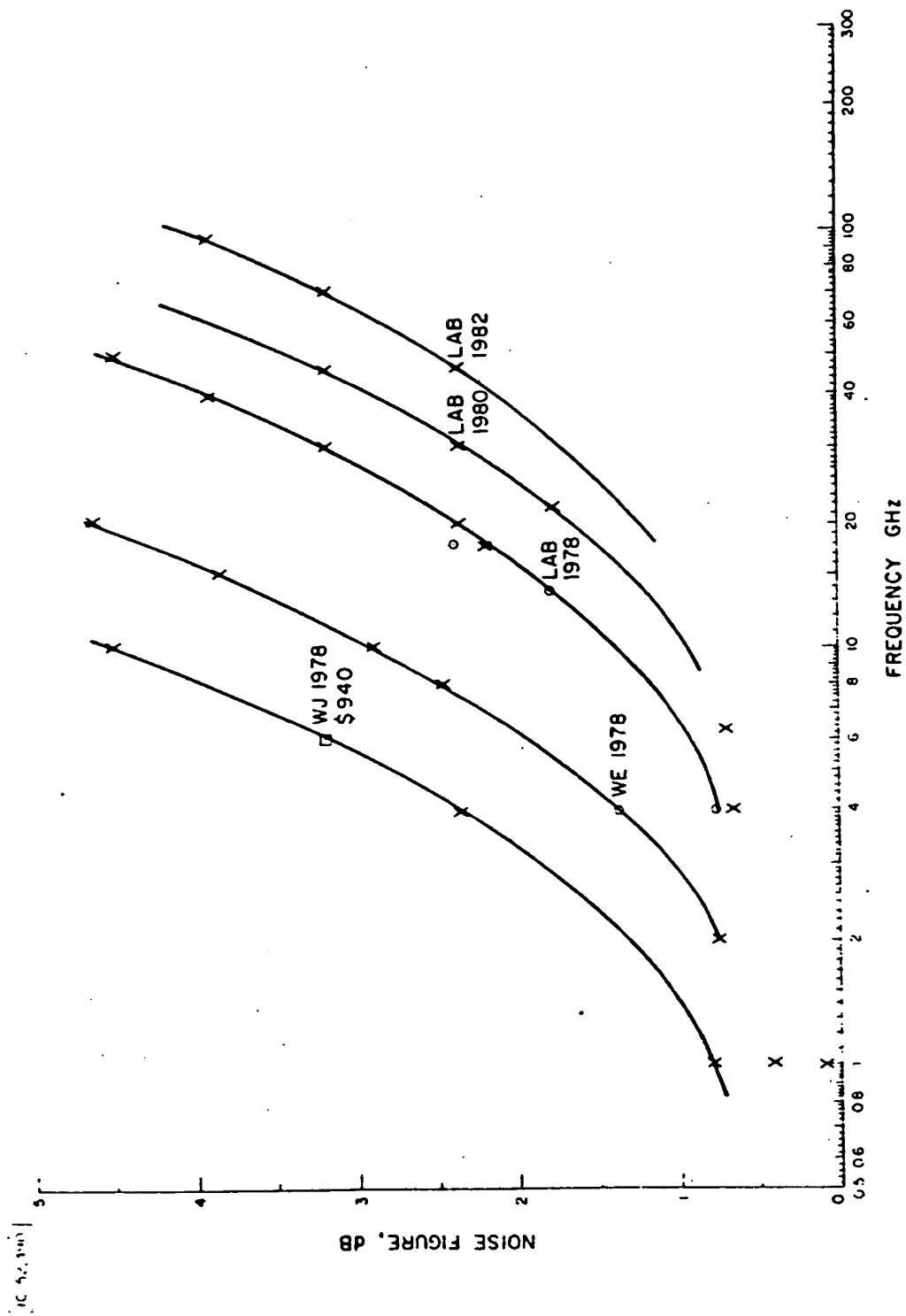
NOISE FIGURE, dB

FREQUENCY GHz

Figure 7. 1978–1982 FET Performance (Actual Data Points Extended by
Fukui Relation, and Frequency Scaled Upward with Time as $10^{t}/9$)

24

Fukui of Bell Laboratories has developed a useful relation for noise figure for GaAs FET's. It is of the form:

$$F = 1 + KfL^{5/6} \left\{ \frac{N}{a} \right\}^{1/6} w^{1/2} \left[r_m + R_{sG} + R_{con} \right]^{1/2} \qquad (10)$$

where

$k \approx 0.033$ = noise coefficient (for good FET's) (1978)

f = frequency in GHz

L = gate length in microns

N = free carrier concentration, x 10^{16} cm^{-3} in active channel

a = active layer thickness under gate in microns

w = unit gate width in microns

r_m = equivalent resistance in the gate itself

R_{sg} = source-to-gate resistance

R_{con} = specific contact resistance

But, by Block & Galage,[15] line width (L) has been decreasing by an order of magnitude every 9 years. This can be seen by examining their figure 2. Another technology (E-beams) is opening which may allow line width to continue decreasing to 0.25 μ. Other observers feel the limit for silicon may be a 0.1 μ, but the limit for GaAs has still not been discussed, to the writers' knowledge. Lepselter of Bell Laboratories (IEEE Spectrum, May 1981) has shown that nearly an order of magnitude drop in channel lengths is possible for MOSFETS, by x-ray lithography. The x-ray lithography has yielded 0.3-0.4 μ gate lengths with good reliability and low expense. Lepselter made a comparison of lithographic techniques based on useful resolution, throughput, exposure system cost, clean room area

25

requirements, and shows that x-ray lithographic methods are two orders of magnitude better than optical lithography, and 1 order of magnitude better than E-beam lithography. The physical limits may be $0.1\,\mu$ rather than $0.25\,\mu$.

We replace (L) in the Fukui relation by $(L_o\, 10^{-t/9})$ to estimate the effect of gate widths as a function of time. Other factors in the equation may also be improved, so the sole effect of an improvement in gate width may give conservative (high) estimates of future noise figures. Figure 7 starts with F = 3 dB @ 26 GHz, F - 1 dB @ 7.2 GHz for estimates of noise figures available in the 1978-1982 period (middle curve labeled Lab '78). Actual 1980 performance is better than that shown, because other improvements have also been made.

The curves on the rights (Lab '80, Lab '82) are estimates of how the Lab '78 curve would improve if gate length is reduced as $10^{-t/9}$ to take advantage of Block and Galage's estimate for improving optical technology and, in this case, E-beam technology. The $0.5\,\mu$ gate length taken for the '78 Lab devices is assumed to become $0.18\,\mu$ in the '82 Lab devices and not other improvements in the FET's are assumed to occur. This may be too conservative an estimate for future performance.

Curves labeled WJ '78 (Watkins-Johnson) and WE '78 (Western Electric) are Fukui curves extended from actual production devices. The Fukui curve effectively says that Western Electric could have produced a 10 GHz FET with 3 dB noise figure if they had desired. The Western Electric curve is also about four years behind the Lab '78 curve. One might guess, by using the Lab '80 curve, that Western Electric could offer 3 dB noise figures at 40 GHz in 1984. A 3.9 dB noise figure at 90 GHz would be possible by 1986 from Western Electric.

Figure 8 shows some recent additions for low noise amplifiers. The dashed line gives the performance of a 0.2 μ gate width FET for comparison.

4.1.1 Power Output

A gross overview of power output as a function of frequency and time has been provided by the March 1978 IEEE Proceedings.[16] Although the capability of solid state devices at 30 GHz has only recently reached an order of one watt, the rate of change is projected at approximately 1-1/2 orders of magnitude per decade. Corresponding average power for tubes is on the order of 100 kilowatts and increasing at a slightly less rapid rate than solid state devices. Power combining[17] techniques are becoming even more effective. In addition, space combining techniques look very promising for phased arrays.

These data suggest the 30/20 GHz or even 40/20 GHz satellite bands will be ripe for commercial exploitation by 1985.

4.1.2 Solid State Antennas

A breakthrough in convenient scanning antennas has occurred recently.[18] Harold Jacobs and his colleagues at USARDC, Fort Monmouth, N.J., used a 13 cm silicon rod with copper foil strips on the top and p-i-n diodes to achieve beam steering at millimeter frequencies. Beam angle changes are typically 8-10 at 63 GHz, and the researchers are attempting to expand the scan angle to 20°.
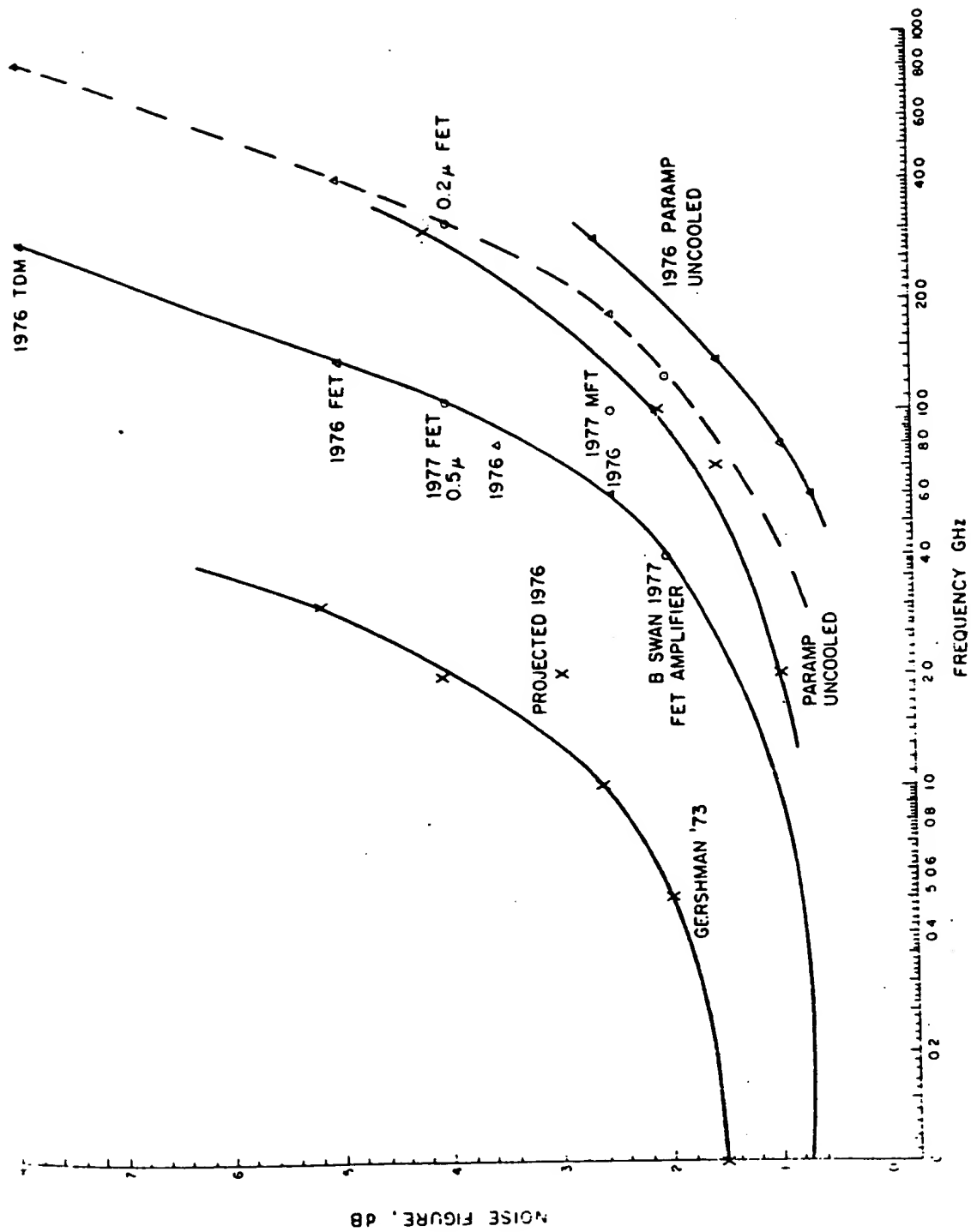
Figure 8. FET and PARAMP Performance

28

SECTION 5

CONCLUSIONS

Useful millimeter wave communication windows were discussed. The Van Vleck gaseous attenuation relations were then listed and unique short closed forms (equation 4 for oxygen and equation 5 for water vapor) were derived for gaseous attenuation on ground-satellite paths. A modified 1979 Crane rain loss model was introduced to find total atmospheric attenuation on a ground-satellite link in the severe Gulf Coast region of Florida. An expotential rain loss probability density function allowed convenient dual diversity loss relation to be found. Then, the possibility of minimizing the sidelobe interference/signal ratio as a function of frequency was discussed and some millimeter frequencies were found attractive (e. g. , figure 3).

The rate of GaAs FET improvement due to decreasing line widths was discussed. This rate of improvement suggested useful devices in the 30/20 GHz satellite bands by 1985, but GaAs FETs are really improving faster than linewidths would suggest. Indeed, the 30/20 GHz bands not only look useful, but may possibly be commercially useful by 1985.

APPENDIX

The received power equation that has usually influenced the reliable satellite link is:

$$P_R = P_t G_t G_R \left(\frac{\lambda_c}{4\pi R}\right)^2 \frac{1}{\ell_a} \frac{1}{\ell_R} \cdots \qquad \text{(A-1)}$$

where

P_R = received power, watts

P_t = transmit power, watts

G_t = power gain of transmit antennas

λ_c = wavelength

R = range

ℓ_a = oxygen plus water vapors $\dfrac{\text{input power}}{\text{output power}}$

ℓ_R = rain loss at specified reliability, $\dfrac{\text{input power}}{\text{output power}}$

This form implies that frequencies less than 10 GHz should be favored when it is noted that ℓ_a and ℓ_R increase sharply with frequency. In this form, however, no emphasis is placed on satellite economics. Instead one can place primary cost emphasis on the system cost studies, either on antenna size directly or use antenna size as a convenient estimate of system

cost. A form of the received power equation which is more consistent with satellite economics can be written as

$$P_R = P_t A_t A_R \left(\frac{1}{\lambda_c R}\right)^2 \frac{1}{\ell_a} \frac{1}{\ell_R} \cdot \qquad \text{(A-2)}$$

where A_t and A_R are effective aperture area. The choice of appropriate units in equations A-1 and A-2 has to be consistent.

For antennas with a radome, Pope[13] has shown relations:

$$\epsilon = \frac{\beta_1 D^{3/2}}{X} \qquad \text{(A-3)}$$

$$\$ = \exp(x - 1) \left[\beta_2 D^{\beta_3} - \beta_4 D^{\beta_5}\right] + \beta_4 D^{\beta/5} \qquad \text{(A-4)}$$

$$G = R \left[\eta \left(\beta_6 Df\right)^2 \exp - \left(\beta_7 \epsilon f\right)^2\right] \qquad \text{(A-5)}$$

where

    ϵ = rms surface tolerance, mm

    D = antenna diameter, ft

    G = absolute antenna gain

    R = radome loss

    f = frequency, GHz

$$\beta_1 = 4.6 \times 10^{-4}; \quad \beta_2 = 6.75 \times 10^{3}; \quad \beta_3 = 1.30$$

$$\beta_6 = 3.20; \quad \beta_7 = 4.19 \times 10^{-2}; \quad \beta = 0.70$$

and, for rigid radomes

$$\beta_4 = 1.28 \times 10^{2}; \quad \beta_5 = 1.85 \quad .$$

The cost ($) equation was seen to depend on both antenna system size (D) and surface tolerance (ϵ). Diameters greater than 15 ft were usually considered by Pope, and cost was a strong function of both diameter and tolerance. As frequency increased, the required tolerance dropped reciprocally and cost increased sharply.

However, interest in small ground terminals (less than 2 meters in diameter) has increased greatly in the past few years. Pope's cost shows only weak dependence on surface tolerance for diameter less than 6-7 feet. This coincides also with recent experience on small machined or precisely formed antennas. This is one reason why link performance at fixed aperture size was emphasized in the body of our report — it has a strong relation to total system cost when small ground antennas are used.

Another analysis has been done (but not shown here) in which antenna diameter was allowed to shrink to maintain constant $ as frequency increased. The resultant gain and S/I performance decreased slightly but did not differ significantly from a constant aperture analysis.

33

REFERENCES

1. D. J. Frediani, "Technology Assessment for Future MILSATCOM Systems: The EHF Bands, "Lincoln Labs Project Report DCA-5, 12 April 1979.

2. W. C. Cummings, P. C. Jain, and L. J. Richardi, "Fundamental Performance Characteristics that Influence EHF MILSATCOM Systems, IEEE Transactions on Communications, Vol. Com 27, No. 10, October 1979, pp. 1423-1435.

3. C. L. Ruthroff, "Multiple-Path Fading on Line-of-Sight Microwave Radio Systems as a Function of Path Lengths and Frequency," Bell System Technical Journal, Vol. 50, No. 7, September 1971, pp. 2375-2398.

4. K. L. Koester, L. H. Kosowsky, "Millimeter Wave Propagation in Fog," IEEE International Antennas and Propagation Symposium, September 1971, Los Angeles, CA.

5. I. Y. Ahmed and L. J. Auchterlonie, "Microwave Measurements on Dust, Using an Open Resonator," Electronics Letters, Vol. 12, 1976, p. 445.

6. J. H. Van Vleck, "The Absorption of Microwaves by Oxygen," Phys. Rev., 71 (7), 1974, pp. 313-324.

7. B. R. Bean and E. J. Dutton, Radio Meteorology, NSB Monograph 92, 1966.

8. P. F. Christopher, "Rain Effects at Random Antenna Elevation," IEEE Trans. Antennas and Propagation (Corres.), Vol. AP-15, pp. 323-324, March 1967.

9. D. O. Reudink, "The Effects of Rain Attenuation on 18/30 GHz Communications Satellite Systems," 1979 Fall URSI Meeting, Seattle, WA.

10. G. Drefuca, "Rain Attenuation Statistics for Frequencies above 10 GHz from Raingauge Observations," J. Rech. Atmos., Vol. 8, pp. 413-420, 1974.

11. R. W. Wilson, "Suntracker Measurements of Attenuation by Rain at 16 and 30 GHz," BSTJ, Vol. 48, No. 5 pp. 1383-1404, May-June 1969.

12. P. F. Christopher, "Orbit Selection for Optimum Satellite System Performance," Proceedings of the 1980 National Telemetry Conference, Houston, TX, 1980.

13. D. L. Pope, "Parametric Representations of Ground Antennas for Communication System Studies," BSTJ, 47 , No. 4, December 1968, pp. 2145-2168.

14. H. Fukui, "Low Noise GaAs MESFETS," Eelectronic Letters, Vol. 12, No. 12, June 1976, pp. 309.

15. E. Block, D. Galage, "Component Progress: Its Effect on High-Speed Computer Architecture and Maching Organization," Computer, April 1978, pp. 64-75.

16. E. J. Nalos, "New Developments in Electromagnetic Energy Beaming," Proc. IEEE, March 1978, Vol. 66, No. 3, pp. 276-288.

17. R. A. Pucel, "Power Combiner Performance of GaAs MESFET," Microwave Journal, 23, No. 3, March 1980, pp. 51-56.

18. H. J. Hindlin, "P-i-n Diodessteer Silicon Antenna," Electronics, September 11, 1980, p. 42: